Inorganic Chemistry

Article

pubs.acs.org/IC

Reactivity Profile of a Peri-Substitution-Stabilized Phosphanylidene-Phosphorane: Synthetic, Structural, and Computational Studies

Brian A. Surgenor, Brian A. Chalmers, Kasun S. Athukorala Arachchige, Alexandra M. Z. Slawin, J. Derek Woollins, Michael Bühl, and Petr Kilian*

School of Chemistry, EaStChem, University of St Andrews, Fife, KY16 9ST, United Kingdom

Supporting Information

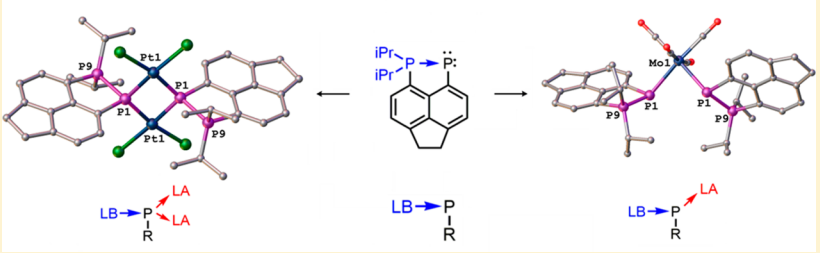

ABSTRACT: The reactions of *peri*-substitution-stabilized phosphanylidene-phosphorane **1** with [AuCl(tht)] or [$PtCl_2$(cod)] afford binuclear complexes [((**1**)$(AuCl)_2)_2$] **2** and [((**1**)$(PtCl_2))_2$] **3**, in which four electrons of the ligand are used in bonding to two metal atoms in the bridging arrangement. Reactions of **1** with [$Mo(CO)_4$(nbd)] or $(RhCl_2Cp^*)_2$ afford mononuclear complexes [$(\mathbf{1})_2Mo(CO)_4$] **4** and [(**1**)$RhCl_2Cp^*$] **5**, in which two electrons of the ligand are used to form terminal complexes. Formation of these complexes disrupts the negative hyperconjugation at the P−P bond to various extents, which is mirrored by variations in their P−P bond distances (2.179(4)−2.246(4) Å). The P−P bond is ruptured upon formation of Pd diphosphene complex **6**, which is likely to proceed through a phosphinidene intermediate. In air, **1** is fully oxidized to phosphonic acid **7**. Reactions of **1** with chalcogens under mild conditions generally afford mixtures of products, from which the trithionated **8**, dithionated **9**, diselenated **10**, and monotellurated **11** species were isolated. The bonding in the chalcogeno derivatives is discussed using DFT (B3LYP) and natural bond orbital analysis, which indicate a contribution from dative bonding in **8**−**10**. The buttressing effect of the *peri* backbone is shown to be an essential factor in the formation of the single push−double-pull bis(borane) **13**. This is demonstrated experimentally through a synthesis parallel to that used to make **13**, but lacking the backbone, which leads to different products. The P−P bond distances in the reported products, as well as additional species, are correlated with Wiberg bond indices, showing very good agreement for a variety of bonding modes, including the negative hyperconjugation.

INTRODUCTION

Phosphinidenes (general formula RP) are six-electron species that are considered to be phosphorus analogues of carbenes. They remain ephemeral, with no condensed-phase example having been isolated other than in cryogenic matrices.[1] Phosphinidenes are ambiphilic (i.e., they can form complexes with either a Lewis acid (LA), a Lewis base (LB), or both). Many complexes with LAs are known, with the most prominent of these being the terminal phosphinidene complexes **A** (Figure 1).[1,2] Examples of "electronically inverse" LB-coordinated species include phosphanylidene-phosphoranes **B**, where a phosphine moiety is coordinated to the phosphinidene unit. Several canonical structures are possible for the latter species, including the dative **B**, ylide **B′**, and ylene **B″** forms.

Phosphanylidene-phosphoranes **B** are known as phospha-Wittig reagents. While the chemistry of Wittig reagents ($R'_3P{=}CR_2$) has been a prominent field of research for many decades, the chemistry of the phosphanylidene-phosphoranes is much less developed, despite being first mentioned in the literature as early as the 1960s.[3] This is due to

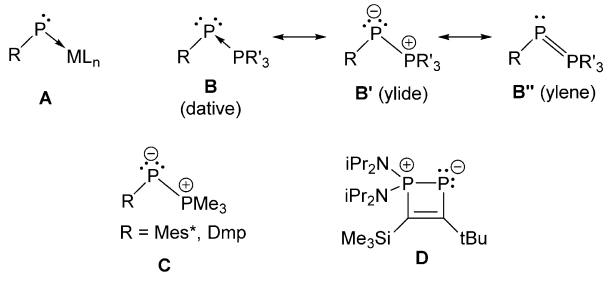

Figure 1. Terminal phosphinidene complexes (**A**), canonical structures of phosphanylidene-phosphoranes (**B**), isolable sterically protected phosphanylidenes (**C**; Mes* = 2,4,6-$tBu_3C_6H_2$, Dmp = 2,6-$Mes_2C_6H_3$), and cyclic electronically and sterically stabilized phosphanylidene (**D**).

Received: March 25, 2014
Published: June 9, 2014

   dx.doi.org/10.1021/ic500697m | *Inorg. Chem.* 2014, 53, 6856−6866

the limited synthetic accessibility of phosphanylidene-phosphoranes, which has resulted in only a handful of isolable (i.e., ambient-temperature stable) species being known.

Nevertheless, phosphanylidene-phosphoranes have received increased attention over the last 15 years, mainly as a result of the activity of Protasiewicz's and Bertrand's groups. Protasiewicz reported two isolable derivatives (**C**), in which the desirable thermal stability was achieved through steric protection of the phosphanylidene atom with very bulky organic groups.[4] Bertrand's group developed a room-temperature stable (cyclic) 1,2-diphosphete (**D**) that achieves stability through a combination of the cyclic structure, electronic stabilization, and steric protection.[5] Various facets of the phosphanylidene-phosphorane chemistry and bonding have been reviewed by Protasiewicz.[6]

In a recent communication,[7] we reported the synthesis and selected reactivity of a new bottleable phosphanylidene-phosphorane, **1**. Our DFT calculations indicate the stability of **1** stems from the buttressing effect of the *peri*-substituted backbone, which locks the phosphine and phosphinidene groups in close proximity. In contrast to all other known phosphanylidene-phosphoranes, the phosphanylidene atom in **1** is rather "naked" (i.e., it is not shielded by any flanking groups). This makes it highly accessible for approach by Lewis acids. We have now exploited this property of **1** in an extensive reactivity study involving a range of electrophiles, which includes transition metal centers (Scheme 1) and chalcogens (Scheme 2). Here, we report our synthetic, spectroscopic, structural, and computational data, with particular emphasis on the supporting role that the backbone plays in the bonding.

RESULTS AND DISCUSSION

Metal Complexes of Phosphanylidene-Phosphorane 1.

Phosphanylidene-phosphoranes contain a Lewis basic two-coordinate phosphorus atom, through which they can act as (overall electroneutral) ligands to coordinate one (η^1) or two (μ^2) Lewis acidic centers, which include transition metals. However, because of the limited number of synthetically accessible phosphanylidene-phosphoranes, only a limited number of complexes has been obtained via direct coordination of the free ligand.

In particular, very few binuclear complexes of the type $R'_3P{\rightarrow}P(R)(\rightarrow LA)_2$ (LA = general Lewis acidic center) have been well-characterized.[8] These include bis(gold) and bis(silver) push−pull complexes formed by the direct reaction of a free phosphanylidene-phosphorane with the appropriate metal center.[8a,b] We have recently expanded this series of binuclear species with the bis(borane) **13** (see Scheme 3),[7] which represents the first structurally characterized main group adduct of this type.

Taking into account the exceptional stability of the bis(borane) push−pull system **13**, we expected a related bis(aurated) complex **2** to be thermally stable. Indeed, the reaction of **1** with AuCl(tht) (tht = tetrahydrothiophene) gave desired complex **2** as a white powder in quantitative yield (Scheme 1). The complex is thermally stable at ambient temperature, although it is rather light-sensitive, as indicated by a color change from colorless to gray when it is exposed to daylight. The ^{31}P NMR spectrum of **2** consists of two doublets (AX spin system, δ_P −44.5 PAu_2; 56.8 ppm, $PiPr_2$, $^1J_{PP}$ 152.0 Hz), with the phosphanylidene atom displaying a remarkably large high-frequency shift upon double coordination to Lewis acidic gold centers (cf. δ_P −157.7 ppm in free ligand **1**).

Scheme 1. Transition Metal Complexes of Ligand 1

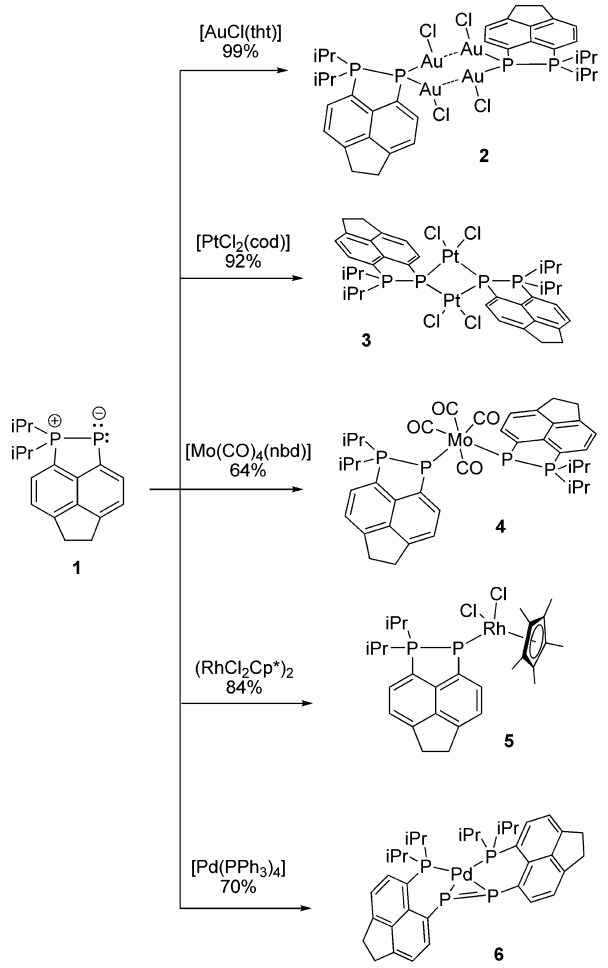

X-ray diffraction revealed that two molecules of **2** associate to form a dimeric assembly in the solid state via Au···Au contacts (3.065 Å, Figure 2). This results in the formation of a twist-boat-shaped P_2Au_4 heterocycle, with the dimer possessing crystallographic C_2 symmetry. The phosphorus atom P1 attains approximate tetrahedral geometry, with the gold atoms adopting a near ideal T-shaped geometry. Coordination to two Lewis acidic gold centers weakens the P−P bond in the ligand to the extent that the P−P bond length in **2** (2.199(7)

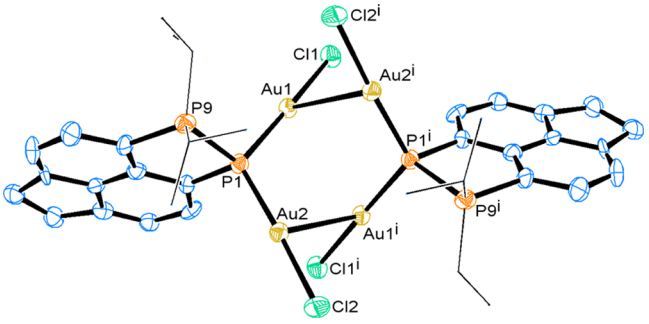

Figure 2. Molecular structure of **2**; two molecules forming a dimeric assembly are shown. Hydrogen atoms and solvated dichloromethane (three molecules) are omitted for clarity. *i*Pr groups are drawn as wireframe for clarity. Selected bond lengths and angles are as follows: P1−P9 2.199(7), P1−Au1 2.248(5), and P1−Au2 2.263(5) Å; Au1−P1−Au2 118.44(18) and P1−Au1−Cl1 174.52(15)°.

dx.doi.org/10.1021/ic500697m | Inorg. Chem. 2014, 53, 6856−6866

Å) is consistent with a single P−P bond (i.e., it is notably elongated versus that in **1**; 2.148(5) and 2.147(6) Å in the two molecules in the asymmetric unit). This is in agreement with the calculated Wiberg bond indices (WBI; 0.89 in **2** and 1.13 in **1** at the B3LYP/SDD/6-31+G* level).[9] The P−Au bond lengths in **2** (2.248(5) and 2.263(5) Å) are comparable to those in the model anionic bridging phosphido complex PPN[$(AuCl)_2(\mu\text{-}PCy_2)$] (2.2481(13) and 2.2440(13) Å, Cy = cyclohexyl, PPN = $(PPh_3)_2N^+$).[10]

A dinuclear platinum complex, **3**, was obtained from the reaction of **1** with $PtCl_2$(cod) (cod = 1,5-cyclooctadiene) in good yield (92%). Insolubility of the complex in common organic solvents prevented measurement of solution NMR spectra and also hindered its purification, although we have been able to obtain crystals suitable for X-ray diffraction work (Figure 3). The molecule of **3** in the crystal possesses a

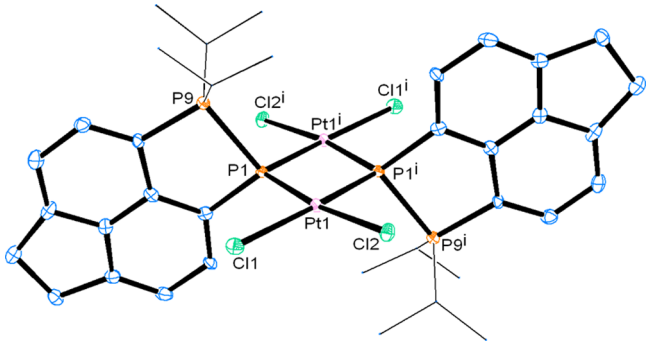

Figure 3. Molecular structure of **3**. Hydrogen atoms and a solvated molecule of dichloromethane are omitted for clarity. *i*Pr groups are drawn as wireframe for clarity. Selected bond lengths and angles are as follows: P1−P9 2.246(4), P1−Pt1 2.239(4), and P1−$Pt1^i$ 2.238(3) Å; Pt1−P1−$Pt1^i$ 103.53(14)°.

crystallographic inversion center located at the midpoint of the P_2Pt_2 ring. The platinum atoms in **3** are *cis*-coordinated, with two μ^2-phosphanylidene ligands oriented *anti* with respect to each other, forming a planar four-membered P_2Pt_2 ring. The P−Pt bond lengths in **3** (2.239(4) and 2.238(3) Å) are very similar to those observed in a related zwitterionic phosphido complex with the P(*cyclo*-$CH_2N(Bn)CHN(Bn)CH_2$) ligand (2.2235(10)−2.2316(11) Å, Bn = benzyl).[11] Despite a slight elongation when compared with **2**, the P−P bond length (2.246(4) Å, WBI 0.84) in **3** is consistent with that of a normal single P−P bond.

Mononuclear phosphanylidene-phosphorane complexes of the general formula $R'_3P{\rightarrow}P(R){\rightarrow}(LA)$ are more common than the dinuclear systems. In particular, they have been exploited as phospha-Wittig reagents by Mathey,[12] and the area was well-reviewed.[6b]

The reaction of $Mo(CO)_4$(nbd) (nbd = norbornadiene) with **1** afforded mononuclear complex **4** as a red solid in 64% yield. The $^{31}P\{^1H\}$ NMR spectrum of **4** displays an AA′XX′ spin system with signals centered at δ_P −104.4 (PMo) and 75.3 ppm ($PiPr_2$). The large magnitude of $^1J_{PP}$ = 430 Hz is notable and is indicative of a strong *peri* P−P interaction (cf. $^1J_{PP}$ 152 Hz in **2** and 201.2 Hz in **13**).

Single-crystal X-ray diffraction shows that the molecule of **4** possesses a (crystallographic) 2-fold axis passing through the Mo atom. Two molecules of **1** act as terminal ligands toward the Mo center (in *cis* fashion). The phosphanylidene donor atoms attain a pyramidal geometry ($\sum$P(1) angles = 322.4°), ruling out any efficient ligand-to-metal π-donation (observed in *planar* phosphido complexes).[13]

Shortening of the P−P bond in the uncoordinated **1** to less than the normal P−P single-bond distance has been ascribed to negative hyperconjugation (i.e., the transfer of electron density from the electron-rich phosphanylidene atom into symmetry-adapted combinations of the P−C σ^* orbitals at the phosphorane center).[6a,14] Interestingly, the P−P distance in Mo complex **4** (2.179(4) Å, WBI 1.00) is rather similar (elongated by only 1.5%) to that in uncoordinated **1** (Figure 4

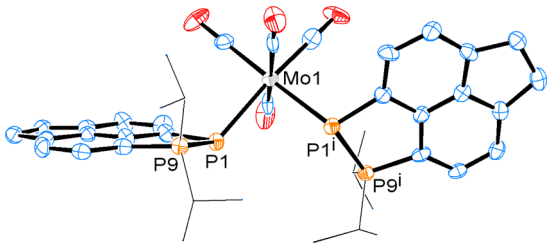

Figure 4. Molecular structure of **4**. Hydrogen atoms and a solvated molecule of chloroform ($^1/_2$ per **4**) are omitted for clarity. *i*Pr groups are drawn as wireframe for clarity. Selected bond lengths and angles are as follows: P1−P9 2.179(4) and P1−Mo1 2.626(4) Å; P1−Mo1−$P1^i$ 87.46(11)°.

Table 1. Selected NMR and Structural Parameters of the *Peri*-Substituted Phosphanylidene-Phosphorane Complexes

	$^1J_{PP}$ (across the *peri* region)	P−P *peri* distance (Å)[a]	WBI [calculated P−P *peri* distance in Å][b]
1	479.6	2.148(5), 2.147(6)	1.13 [2.165]
13	201.2[c]	2.208(11)[c]	0.94 [2.260]
2	152.0	2.199(7)	0.88 [2.263][d]
3		2.246(4)	0.84 [2.289]
4	430.0	2.179(4)	1.00 [2.205]
5	452.4	2.198(10)	0.93 [2.257]
6	32[e]	3.24, 3.19	0.08 [3.248][f]

[a]Experimental P−P distance (from X-ray diffraction). [b]B3LYP/SDD/6-31+G* level; for details, see Computational Details in the Experimental Section. [c]From ref 7. [d]Very similar values are obtained for the monomeric structure (i.e., (**1**)(2AuCl)) or when the Au···Au distances are fixed to the X-ray values. [e]$^2J_{PP}$. [f]The side-coordinated P═P bond in the Pd complex has a WBI of 1.30.

and Table 1). This indicates that some degree of negative hyperconjugation may be preserved in **4** despite one of its lone pairs being sequestrated via bonding to the Mo center. A similar observation was made in zwitterionic triphosphenium transition metal complexes, where coordination of a single metal fragment to the central two coordinate phosphorus atom resulted in only modest elongation of the P−P bonds, which thus retained some of their partial double character.[15] It is worth mentioning that transition metal η^1-complexes of diphosphenes, which possess conventional π−π (double) bonds, also show minimal elongation upon coordination of the lone pair of the phosphorus atom to the metal.[16]

Red−brown complex **5** was obtained in good yield (84%) from the clean reaction of $[RhCl_2Cp^*]_2$ with **1**. The $^{31}P\{^1H\}$ NMR spectrum of **5** consists of two doublets of doublets (AM part of AMX spin system, A and M = ^{31}P, X = ^{103}Rh), centered

dx.doi.org/10.1021/ic500697m | *Inorg. Chem.* 2014, 53, 6856−6866

at δ_P 11.8 (PRh) and 70.9 ppm (P*i*Pr$_2$). The observed magnitude of the $^1J_{PP}$ is large (453 Hz) and consistent with the expected terminal coordination of **1**. As expected, the ^{103}Rh splitting of the former signal ($^1J_{PRh}$ = 102 Hz) is much larger than that of the latter one ($^2J_{PRh}$ = 3.5 Hz). Notable is the dissimilarity of the chemical shifts of the phosphanylidene atoms in **4** and **5** ($\Delta\delta_P$ 116.2 ppm). The ^{1}H and ^{13}C NMR spectra are fully consistent with terminal coordination of a single phosphanylidene-phosphorane ligand to a Rh center.

Despite our repeated efforts using a variety of solvents and crystallization techniques, we have been able to grow only low-quality crystals of **5**. Hence, our structural data are rather poor; however, they are adequate to demonstrate connectivity and to provide additional support for the assignment of the structure from the NMR data. The structural data indicate a pyramidal geometry around the phosphorus donor atom, and our calculations show that the P−P bond in the fully optimized structure has a WBI of 0.93 (Figure 5 and Table 1).

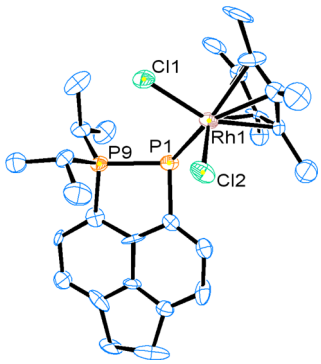

Figure 5. Molecular structure of **5**. Hydrogen atoms and a solvent molecule of thf are omitted for clarity. Structural data are of limited accuracy because of the low quality of the crystal.

The structural and spectroscopic data indicate that in all of the above complexes (**2**−**5**) the phosphanylidene-phosphorane ligand displays phosphido-like coordination (either bridging or a pyramidal terminal mode). This is in agreement with the notion that the ylide mesomeric structure (**B**′ in Figure 1) best describes the bonding in **1**; in this form, the phosphorus atom P1 possesses two lone pairs and carries a formal negative charge. It appears that the zwitterionic nature of free ligand **1** (i.e., its overall neutral, rather than negative, charge as in phosphido ligands) has little bearing on its binding to metal centers, for which both P1's lone pairs can be used. An interesting facet of the bonding in these complexes is their formal push−pull character. In the case of **2** and **3** (and **13**), the bonding can be seen as a push−double-pull structure LB→PR(→LA)$_2$, whereas in **4** and **5**, the bonding LB→PR→LA formally involves push−pull donor−acceptor interactions as well as an additional lone pair on the central atom.

The reaction of **1** with [Pd(PPh$_3$)$_4$] yielded Pd^0 complex **6**, whose synthetic and structural details were reported in our recent communication.[7] In **6**, the phosphanylidene-phosphorane ligand displays a coordination behavior distinct to that seen in the terminal and bridging phosphido-like complexes mentioned above. Instead, the phosphine donor-phosphinidene acceptor aspect of bonding (see **B** in Figure 1) is highlighted. At least formally, the sequestration of the phosphine donor's lone pair by the Pd metal center results in the formation of a free phosphinidene moiety, which readily undergoes dimerization to form a diphosphene. The formed diphosphene group is η^2-bonded to the palladium center to give 16-electron complex **6**.

Notably, the formation of **6** is distinct from another metal-induced P−P bond-breaking reaction of phosphanylidene-phosphorane reported in the literature, namely, the phosphinidene group transfer to low-valent early transition metals, which yields terminal phosphinidene complexes.[17]

Reactions of Phosphanylidene-Phosphorane 1 with Chalcogens. Because of the very low valence state of the phosphanylidene atoms, phosphanylidene-phosphoranes have been recognized as valuable precursors for phosphorus compounds in a variety of oxidation and coordination states. Bertrand's rigid 1,2-diphosphete served as a precursor to a range of species, where the coordination number of the phosphanylidene atom was increased from 2 to 3, 4, 5, and 6. Interestingly, in all of these species, the P−P bond (i.e., the cyclic structure) was preserved as long as the crowding in the ethylenic part of the ring was present.[18]

In contrast to Bertrand's 1,2-diphosphete system, our 5,6-acenaphthene framework displays more flexibility. Thus, in addition to a range of (cyclic) P−P bonded species, **9**−**11**, P−S−P bridged compound **8** as well as acyclic phosphonic acid **7** were obtained from the reactions of phosphanylidene-phosphorane **1** with chalcogens and air, respectively (Scheme 2).

Scheme 2. Chalcogenides Derived from 1

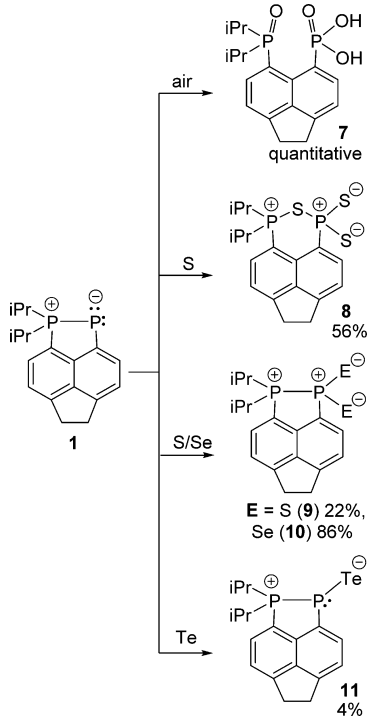

Exposure of a solution of **1** in MeCN to air led to discoloration of the initially red solution and later to slow formation of colorless crystals of the phosphonic acid **7**. The thus collected material was of analytical purity; in addition to microanalysis, the acid was fully characterized by X-ray diffraction (Figure 6), HRMS, and IR. Because of its insolubility in common solvents, we could not obtain any solution NMR spectra of **7**. Titration of **7** with KOH afforded water-soluble

dx.doi.org/10.1021/ic500697m | Inorg. Chem. 2014, 53, 6856−6866

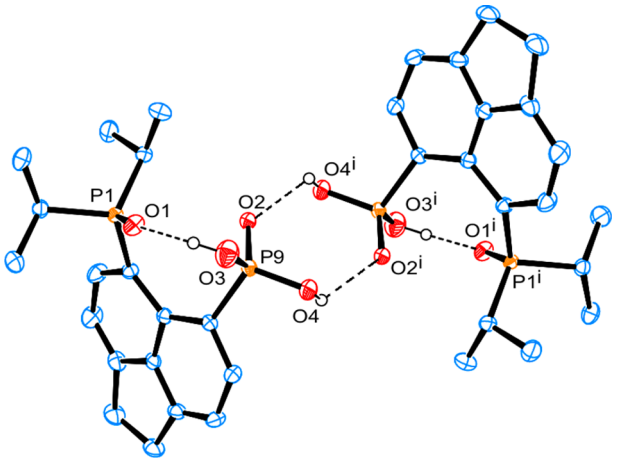

Figure 6. Molecular structure of **7**; two molecules bound by hydrogen bonds (dashed lines) are shown. Carbon-bound hydrogen atoms are omitted for clarity. Selected bond lengths and angles are as follows: P1−O1 1.501(2), P9−O2 1.493(2), P9−O3 1.524(2), P9−O4 1.548(2), and P1···P9 3.58 Å; O3−H3···O1 161(1) and O4−H4···O2^{i} 117(1)°.

dipotassium salt **7a**, which was subsequently fully characterized by multinuclear NMR, Raman, and IR.

The room-temperature reaction of **1** with powdered sulfur in toluene gave a mixture of products, as shown by ^{31}P NMR. Varying the stoichiometry, solvent, and reaction temperature led to the formation of identical products in essentially the same ratio. The mixture was separated using column chromatography, which gave two analytically pure products, **8** and **9**, in 56 and 22% yields, respectively. Both **8** and **9** were fully characterized, and their crystal structures were determined (Figure 7). After purification, **8** was not soluble in any common

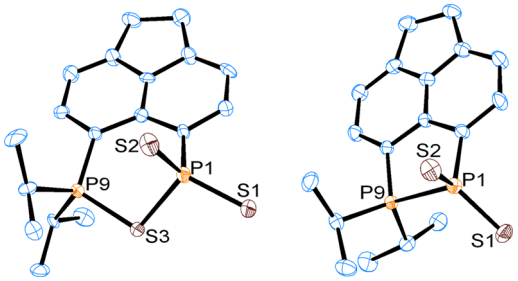

Figure 7. Molecular structures of **8** (left) and **9** (right). Hydrogen atoms are omitted for clarity. Selected bond lengths and angles (values in square brackets are for second molecule within the asymmetric unit; only one molecule is shown in each figure) are as follows for **8**: P1−S3 2.172(3) [2.180(3)], P9−S3 2.025(3) [2.083(3)], P1−S1 1.943(3) [1.987(3)], and P1−S2 1.984(3) [1.924(3)] Å; P1−S3−P9 101.51(11) [99.60(11)]°; for **9**: P1−P9 2.2753(14) [2.2910(15)], P1−S1 1.9619(15) [1.9621(14)], and P1−S2 1.9601(15) [1.9606(15)] Å.

organic solvent, which prevented direct measurement of its solution NMR spectra. The solid-state ^{31}P{^{1}H} MAS NMR spectrum of **8** (162.0 MHz) displayed two singlets at δ_P 69.8 and 59.4. Comparison to solid-state NMR data and the observed integral intensities allowed assignment of the peaks in the solution NMR spectrum of the crude mixture after the reaction of **1** with sulfur: signals at δ_P 73.8 (d, -PS$_3$) and 55.5 (d, -PS(*i*Pr)2), $^{2}J_{PP}$ = 9.4 Hz, were identified as belonging to **8**.

Mild conditions (ambient temperature) were sufficient to drive the reaction of **1** with powdered gray selenium to completion. Analytically pure diselenated species **10** was isolated in very good yield (86%) after purification by column chromatography and was fully characterized, including single-crystal X-ray diffraction (Figure 8).

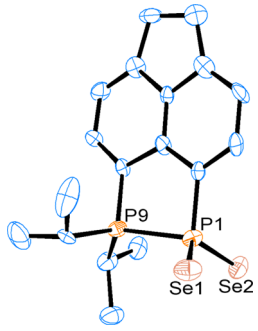

Figure 8. Molecular structure of **10**. Hydrogen atoms are omitted for clarity. Selected bond lengths and angles (values in square brackets are for second molecule within the asymmetric unit; only one is shown in figure) are as follows: P1−P9 2.342(6) [2.303(6)], P1−Se1 2.116(4) [2.132(5)], and P1−Se2 2.136(4) [2.129(5)] Å.

To complete the series of chalcogenides, the reaction of **1** with powdered tellurium was performed in boiling toluene. A complex mixture was obtained, as indicated by ^{31}P NMR. A minute amount of red platelet crystals of **11** was obtained via recrystallization from toluene. Their identity was confirmed by single-crystal diffraction (Figure 9); however, the small quantity

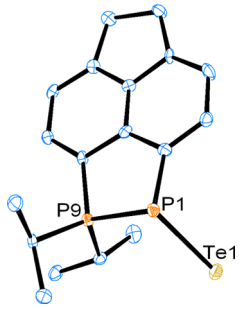

Figure 9. Molecular structure of **11**. Hydrogen atoms are omitted for clarity. Selected bond lengths and angles are as follows: P1−P9 2.225(3) and P1−Te1 2.4256(17) Å; P9−P1−Te1 107.56(9)°.

of material available, combined with thermal decomposition (observed as darkening of the solutions of **11** via elimination of elemental tellurium), prevented any further characterization.

Discussion of Bonding in 7−11. The crystal structure of **7** (Figure 6) indicates that all oxygen atoms are involved in hydrogen bonding. Thus, a pair of intermolecular O4−H4···O2′ and O4′−H4′···O2 bonds leads to formation of dimeric assemblies; the remaining interaction (O3−H3···O1) is intramolecular.

The most prominent feature in the crystal structure of **8** (Figure 7) is the dissimilarity of the bridging P−S bond lengths (S3−P9 2.025(3) and S3−P1 2.172(3) Å). This may indicate the partial dative character of bonding (see resonance structure **8′** in Figure 10), akin to the situation observed in the related structure Nap[PCl$_2$(=O)][PCl$_4$] (Nap = naphthalene-1,8-diyl),[19] or may simply mirror the differing electronic and steric

dx.doi.org/10.1021/ic500697m | *Inorg. Chem.* 2014, 53, 6856−6866

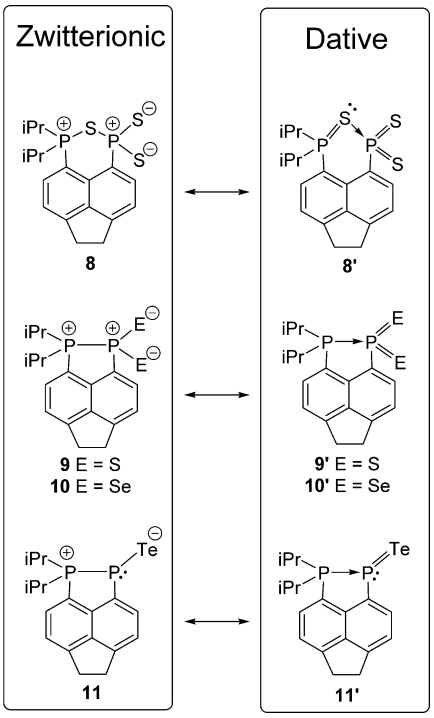

Figure 10. Resonance structures of the chalcogenides.

attributes of the two phosphorus environments. Our WBI and natural charge calculations support the dative interpretation of bonding; they indicate the WBIs in the fully optimized structure of **8** are 0.53 (S3−P1) and 1.13 (S3−P9), whereas calculated natural charges are −0.33 (S3), 0.91 (P1), 1.41 (P9), and −0.53 on each of the terminal S atoms.

Despite the observed difference in strength of S3−P1 bond (weaker) versus the S3−P9 (stronger) bond, the localized MO structure obtained from a natural bond orbital (NBO) analysis[20] contains two σ-bonding MOs with high occupancy (>1.94) for these two bonds. Only single P−S bonds are found in this analysis, together with two lone pairs on S3 and three on each of the S1 and S2 atoms, which would seem to support the zwitterionic resonance structure **8** (Figure 10). However, in a second-order perturbation theory analysis of donor−acceptor interactions,[20] significant delocalization of one of the lone pairs on S3 into a P9−C antibonding orbitals is apparent, in line with the partial double-bond character inferred for the S3−P9 bond from its length and WBI. As typical for delocalized and dative bonds, the true situation is a hybrid between resonance structures shown in Figure 10 (top).

The two limiting mesomeric structures shown at the middle of Figure 10 are of particular relevance to the description of the bonding in **9** and **10**. These are a covalent zwitterionic structure and a Lewis acid−base complex of the phosphine donor group (-P*i*Pr$_2$) with a coordinatively unsaturated metaphosphonate functionality (-P(=S)$_2$). Correspondingly, tellurium derivative **11** has two mesomeric structures, as shown in Figure 10 (bottom). Although the P−P distances in **9** (2.2753(14) and 2.2910(15) Å) and **10** (2.342(6) and 2.303(6) Å) indicate a weakened P−P bond,[21] potentially indicating contributions from the dative bonding (see structures **9′** and **10′** in Figure 10), tellurium derivative **11** has a P−P bond length (2.225(3) Å) that is in the middle of the normal P−P single-bond range, as would be expected for the zwitterionic structure **11** (see Figure 10). This is further supported by the computed P−P bond WBIs, which have values of 0.62−0.63 for **9** and **10** (indicating significantly weakened single bonds) and 0.84 for **11** (close to a full single bond). In contrast, NBO analysis indicates all minima are characterized by P−P and P−E σ-bonds with three lone pairs on each chalcogen, suggesting a predominance of the zwitterionic over the dative structures.

It should be noted that several intramolecular donor-stabilized metaphosphonates (LB→P(=S)$_2$R) as well as metaphosphinites (LB→P(=S)R) were reported by Yoshifuji (LB = dimethylamino group)[22] and by us (LB = diisopropylphosphino group).[23] Just like that for **9**−**11**, the donor stabilization is rather efficient in these literature species, as some of the derivatives were inert enough to be purified by column chromatography.

An interesting observation from the reactions with chalcogens is that they proceed under relatively mild conditions, indicating that **1** is rather reactive in comparison to (for example) tertiary phosphines or cyclic oligophosphines.[24] In line with decreasing oxidizing power of elements on going down group 16, lower oxidation state phosphorus centers become more prevalent at the bottom of the group.

General Bonding Considerations. The P−P bonding is remarkably variable within the reported new compounds, with computed WBIs in the range of 0.62−1.30. These WBIs correlate well with optimized P−P distances as shown in Figure 11. For completeness, we have extended the correlation toward

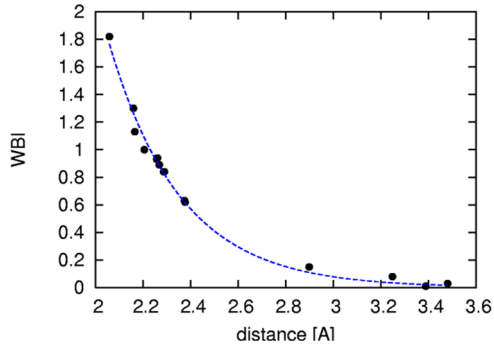

Figure 11. Plot of computed WBIs vs the P−P bonded and nonbonded distances (B3LYP level); data points represent species listed in Tables 1 and S1 (see the Supporting Information). The dashed line shows an exponential fit to all points.

hypothetical Ph−P=P−Ph as well as to nonbonded P···P interactions; for details, see Table S1 in the Supporting Information. The resulting extended correlation confirms WBI structural parameter as a useful tool to quantify the combination of σ, π, and negative hyperconjugation bonding.

Further Synthetic Studies Related to Phosphanylidene-Phosphorane 1. *Alternative Reduction of 12 to 1.* Only a few stable phosphanylidene-phosphoranes have been reported in the literature, and the majority of the synthetic pathways leading to these species appear to be highly specific and not of general applicability. The exception to this is the reduction of dichlorophosphines with a synergistically acting zinc and PMe$_3$ reducing reagent. The procedure was originally introduced by Mathey for metal-assisted phospha-Wittig chemistry,[25] and then it was further developed by Protasiewicz, who used it to synthesize the bulky bottleable phosphanylidene-phosphoranes DmpP=PMe$_3$ and Mes*P=PMe$_3$ (**C**).[6b] The scope of this reaction was broadened to incorporate other trialkylphosphines (PEt$_3$ and PBu$_3$), although further expansion

dx.doi.org/10.1021/ic500697m | Inorg. Chem. 2014, 53, 6856−6866

toward species with less bulky groups at phosphanylidene atom was not successful. The reaction scope was appropriately described as "a limited window of synthetic viability towards the isolation of free phosphanylidenephosphoranes";[6b] this notwithstanding, it appeared to be of interest to challenge this notion with respect to our *peri*-substituted system.

It should be noted that the high yielding and convenient synthesis of phosphanylidene-phosphorane **1** from phosphine-phosphine complex **12** was reported by us recently (see Scheme 3, top reaction).[7] This synthesis, utilizing bis(borane)

Scheme 3. Reduction of 12 with BH_3·SMe_2 and with Zinc Powder

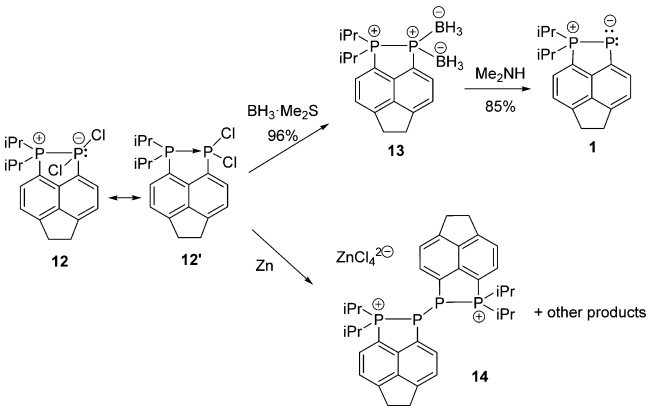

13 as an intermediate, represents a fundamentally new addition to the (very limited) collection of synthetic routes toward phosphanylidene-phosphoranes.

Nevertheless, to examine whether **1** is accessible by the alternative (Protasiewicz's) pathway, we reacted **12** with zinc powder. The molecule of **12** possesses (at least formally) both of the required phosphine components: the dichlorophosphino group ($ArPCl_2$) and the (highly basic) tertiary phosphino group ($ArPiPr_2$) (see dative resonance form **12′** in Scheme 3). These are conveniently prearranged in close proximity by means of the rigid backbone, giving rise to a phosphonium-phosphoranide zwitterionic form (**12** in Scheme 3). Therefore, addition of powdered zinc to **12** can be considered as an intramolecular variation of the Protasiewicz's protocol.

However, the reaction of **12** with zinc gave inconclusive results. Despite repeating the reaction in a variety of solvents and at different temperatures, formation of **1** was not observed in the ^{31}P NMR spectra of the mixtures after the reaction. On the other hand, a small amount of the ionic species, **14**, was obtained via recrystallization of the crude mixtures from MeCN. The identity of **14** was confirmed by single-crystal X-ray diffraction (Figure 12). Formation of the $ZnCl_4^{2-}$ anion and the 1,4-diphosphonium dication (seen in **14**) indicates that the reduction of the dichlorophosphino group takes place. However, zinc is not a strong enough reductant to reduce **12** as far as to **1** (**1** is formally a product of the two-electron reduction of **14**), although this interpretation is tentative because **14** is likely to be only a minor component of the product mixture, whereas the other products remain unknown. An X-ray structure of a compound related to **14** (with the same dication but two chloride counterions) was reported by us earlier and shows similar metric parameters.[26]

Demonstration of a Novel Reactivity Brought about by the Forced Proximity Effect. The reaction of **12** with BH_3·SMe_2 gives bis(borane) **13** in quantitative yield (Scheme 3). Although a few monoborane adducts of phosphanylidene-phosphoranes are known, formation of the bis(borane) adduct is much less common, and the air-stable nature of **13** is unique.[6a,7]

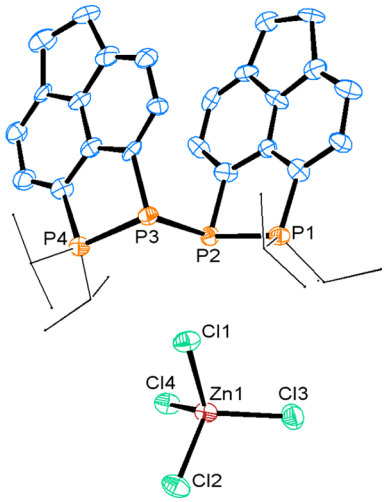

Figure 12. Molecular structure of **14**. Hydrogen atoms and solvated acetonitrile (2 molecules) are omitted for clarity. *i*Pr groups are drawn as wireframe for clarity. Selected bond lengths and angles are as follows: P1–P2 2.243(6), P3–P4 2.240(6), and P2–P3 2.287(6)Å; P1–P2–P3–P4 157.89(17)°.

We hypothesized that the forced proximity of the two phosphorus functionalities, brought about by placing them at the *peri* positions in acenaphthene, plays a key role in stabilization of this push–double-pull motif. However, while computational methods gave some insight into this,[7] no direct experimental proof has been available so far.

In a search for such evidence, we have performed a reaction analogous to that used to make **13**, using closely electronically and sterically related components that, however, were not coupled together by the acenaphthene backbone (Scheme 4).

Scheme 4. Attempted Preparation of Uncoupled Bis(borane) 15

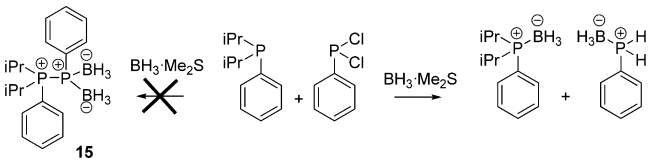

To an equimolar mixture of the two independent halves ($PhPCl_2$ and $PhPiPr_2$) was added an excess of Me_2S·BH_3 rapidly (to parallel the conditions used in the preparation of **13**;[7] the reaction is depicted in Scheme 3). The $^{31}P\{^1H\}$ NMR spectrum of the mixture after the reaction showed that monoborane adducts $PhPiPr_2$·BH_3 and $PhPH_2$·BH_3 were the sole phosphorus-containing products of the reaction. No push–pull product **15** (see Scheme 4) was detected by ^{31}P NMR in the mixture after the reaction. The result of this experiment strongly supports the notion that the unique reactivity leading to push–pull bis(borane) **13** is indeed a result of the *peri*-preorganization effect. In a more general sense, this experiment provides additional evidence that *peri* substitution supports unique reactivity and structure in a variety of environments.

dx.doi.org/10.1021/ic500697m | *Inorg. Chem.* 2014, 53, 6856–6866

CONCLUSIONS

Phosphanylidene-phosphorane **1** has been shown to act as a robust two (η^1) or four (μ^2) electron phosphido-like donor toward transition metal centers via its low-valent phosphorus donor atom. The P−P bond (of variable strength) is preserved in these complexes. Additionally, the phosphinidene-like reactivity has been observed in the formation of **6**. Here, the phosphinidene-phosphorane ligand reorganizes into the diphosphene dimeric assembly, which provides six electrons overall for bonding with the palladium center.

1 provides a rigid framework for a variety of chalcogen species; the bonding analysis, supported by availability of a range of crystal structures and using computational methods (WBI, NBO), indicates contributions from both zwitterionic and dative bonding in compounds **8**−**10**, but less so in **11**.

The P−P bond lengths vary remarkably within the two groups of reported compounds; in some cases, negative P−P hyperconjugation is present, leading to shorter than single-bond distances. The P−P interaction mirrors the amount of electron density sequestrated by the Lewis acidic metal centers or by chalcogen atoms. A correlation of computationally obtained WBIs versus bond length (extended toward "genuine" $\pi-\pi$ bonds and sub van der Waals interactions) is given, showing a very good fit.

Reaction of the dichloride **12** using Protasiewicz's standard procedure (with Zn powder) did not give any phosphanylidene-phosphorane **1**. On the other hand, **1** is readily accessible in very good yields via reduction with borane dimethylsulfide adduct (a route developed by us). This indicates that the nature of the reducing reagent is crucial, and optimization of this aspect may lead to synthesis of new derivatives.[27]

The different outcome of the reduction of the closely structurally and electronically similar species lacking the *peri* backbone confirms that the proximity effects synonymous with *peri* interaction do indeed modify the reactivity and are a crucial aspect in the formation of bis(borane) **13**.

EXPERIMENTAL SECTION

General Procedures. All reactions and manipulations were performed with exclusion of air and moisture under an atmosphere of N_2 or Ar using standard Schlenk and glovebox techniques unless otherwise stated. Solvents were dried on an MBraun solvent purification system and stored over molecular sieves prior to use. **1**,[7] **12**,[26] and $PtCl_2(cod)$[28] were prepared according to literature procedures; all other chemicals were obtained from commercial sources and were used as obtained. NMR measurements were performed at 25 °C; the spectra are referenced to 85% H_3PO_4 in ^{31}P, TMS in ^1H and ^{13}C, and Me_2Se in ^{77}Se NMR. Where possible, new compounds were fully characterized by ^{31}P, $^{31}P\{^1H\}$, ^1H, and $^{13}C\{^1H\}$ NMR, including measurement of $^1H\{^{31}P\}$, H−H DQF COSY, H−P HMQC, H−C HSQC, and H−C HMBC experiments. The NMR numbering scheme is shown in Figure 13. Thermal ellipsoids in all ORTEP figures are set at 40% probability.

CCDC 961463−961471 and 993005 contain the supplementary crystallographic data for this paper. These data can be obtained free of charge via www.ccdc.cam.ac.uk/data_request/cif, or by e-mailing data_request@ccdc.cam.ac.uk, or by contacting The Cambridge Crystallographic Data Centre, 12 Union Road, Cambridge CB2 1EZ, UK; fax: +44 1223 336033.

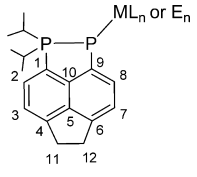

Figure 13. General NMR numbering scheme.

Gold Complex 2. To a stirred suspension of [AuCl(tht)] (0.21 g, 0.66 mmol) in toluene (10 mL) at −10 °C was added a deep red solution of **1** (100 mg, 0.33 mmol) in toluene (10 mL) dropwise with stirring, which resulted in a yellow suspension. After stirring for 30 min, the solid was collected by filtration using sinter and was dried in vacuo (in the dark), giving **2** as a white powder (250 mg, 0.163 mmol, 99%). Crystals of **2** suitable for X-ray diffraction were obtained from CH_2Cl_2. The solid initially dissolves in chlorinated solvents but instantly crystallizes out, which prohibited obtaining ^1H and ^{13}C NMR data. **2** decomposes rather rapidly turning purple and then gray when exposed to light. Anal. Calcd for $C_{36}H_{44}P_4Au_4Cl_4$: C, 28.25; H, 2.90. Found: C, 27.99; H, 3.02. $^{31}P\{^1H\}$ NMR (121.5 MHz, mixture after the reaction in toluene): δ_P −44.5 (d, PAu_2), 56.8 (d, $P(iPr)_2$), $^1J_{PP}$ = 152.0 Hz.

Platinum Complex 3. To a stirred suspension of [$PtCl_2$(cod)] (187 mg, 0.5 mmol) in thf (10 mL) was added a solution of **1** (150 mg, 0.5 mmol) in thf (15 mL) slowly. The mixture was stirred overnight, producing a pale yellow solution. The solvent was then evaporated in vacuo to $^1/_4$ of its initial volume, and pentane (5 mL) was added, producing an off-white precipitate. The precipitate was collected by filtration and dried in vacuo to give **3** as an off white powder (520 mg, 0.46 mmol, 92%). The compound is insoluble in common organic solvents; however, a small amount of crystals suitable for X-ray diffraction was obtained by cooling of the warm supernatant from DCM extracts of **3**.

Molybdenum Complex 4. To a stirred solution of [Mo(CO)$_4$(nbd)] (151 mg, 0.5 mmol) in toluene (10 mL) at −10 °C was added a solution of **1** (300 mg, 1.0 mmol) in toluene (10 mL) slowly, and the mixture was warmed to room temperature and stirred overnight. The solution was concentrated to $^1/_4$ of its initial volume in vacuo, which led to the precipitation of a brown solid. This was collected by filtration, washed with diethyl ether (2 × 5 mL), and dried in vacuo to give **4** as a deep red powder (255 mg, 0.32 mmol, 64%). Anal. Calcd for $C_{40}H_{44}O_4P_4Mo{\cdot}2CH_2Cl_2$: C, 51.55; H, 4.94. Found: C, 51.02; H, 4.95. ^1H NMR (300.1 MHz, CD_2Cl_2): δ 1.17−1.43 (m, 8 × CH_3), 2.70−3.07 (m, 4H, 4 × CH at *i*Pr), 3.13−3.63 (m, 4 × CH_2), 7.20−7.31 (m, 2H, $^3J_{HH}$ = 7.1, H7), 7.43 (br d, 2H, $^3J_{HH}$ = 6.8 Hz, H3), 7.74 (t, $^3J_{HP}$ = $^3J_{HH}$ = 7.4 Hz, 2H, H2), 8.07 (m, $^3J_{HH}$ = 7.1 Hz, 2H, H8). $^{13}C\{^1H\}$ NMR (75.5 MHz, CD_2Cl_2) δ 18.4 (d, $^2J_{CP}$ = 7.3 Hz, 8 × CH_3), 26.6 (dd, $^1J_{CP}$ = 34.7, $^2J_{CP}$ = 6.1 Hz, 4 × CH at *i*Pr), 32.2 (s, CH_2, C12), 33.5 (s, CH_2, C11), 120.0−121.0 (m, C1), 121.5 (d, $^3J_{CP}$ = 9.2 Hz, C3), 123.2−124.0 (m, C7), 128.8−130.8 (m, C8), 132.1 (s, C2), 139.4 (d, $^3J_{CP}$ = 11.7 Hz, C5), 140.4 (d, $^2J_{CP}$ = 23.2 Hz, C10), 142.0 (s, C6), 148.6 (dd, $^1J_{CP}$ = 36.6, $^2J_{CP}$ = 8.6 Hz, C9), 154.0 (s, C4), 187.3 (d, $^2J_{CP}$ = 15.1 Hz, CO), 203.6 (d, $^2J_{CP}$ = 13.3 Hz, CO), 214.9 (s, CO), 221.6−223.2 (m, CO). $^{31}P\{^1H\}$ NMR (121.5 MHz, CD_2Cl_2): AA′XX′ spin system: δ −104.4 (P(Mo), P^A), 75.3 ($P(iPr_2)$, P^X), $^1J(P_AP_X)$ = 430 Hz, $^2J(P_AP_{A'})$ = 220 Hz, $^3J(P_AP_{X'})$ = $^3J(P_{A'}P_X)$ = −48 Hz, $^4J(P_XP_{X'})$ = 3 Hz. Raman (glass capillary, cm^{-1}): ν 3068m (νAr−H), 2933m, 2887w (νC−H), 1989m, 1871m, 1826m (νC≡O), 1610s, 1445m, 1416vs, 1388m, 1345w, 843m, 722m, 462vs, 428s. Crystals for X-ray work were grown from chloroform.

Rhodium Complex 5. To a stirred solution of $(RhCp^*Cl_2)_2$ (0.20 g, 0.327 mmol) in toluene (20 mL) was added a solution of **1** (0.196 g, 0.653 mmol) in toluene (10 mL) dropwise at room temperature. The mixture instantly turned deep brown and was allowed to stir overnight. The resulting suspension was filtered, and the solid obtained was dried in vacuo to give **5** as a deep red−brown solid (334 mg, 0.548 mmol, 84%). ^1H NMR (300.1 MHz, $CDCl_3$): δ 1.11 (dd, $^3J_{HP}$ = 19.2 Hz, $^3J_{HH}$ = 6.9 Hz, 6H, 2 × CH_3 at *i*Pr), 1.23 (dd, $^3J_{HP}$ = 16.5 Hz, $^3J_{HH}$ = 7.1 Hz, 6H, 2 × CH_3 at *i*Pr), 1.65 (s, 15H, 5 × Cp* CH_3), 3.16−3.52 (m, 6H, 2 × CH at *i*Pr and 2 × CH_2), 7.23 (br d, $^3J_{HH}$ = 8.2 Hz 1H, H7), 7.33 (br d, $^3J_{HH}$ = 7.1 Hz, H3), 7.37−7.51 (m,1H, $^3J_{HH}$ = 7.1 Hz, H8), 7.61 (t, $^3J_{HP}$ = $^3J_{HH}$ = 7.2 Hz, 1H, H2). ^{13}C NMR (75.5 MHz, CD_2Cl_2) δ 9.8 (s, 5 × Cp* CH_3), 17.7 (s, 2 × CH_3), 18.2 (s, 2 × CH_3), 25.0 (s, CH at *i*Pr), 25.2−25.7 (m, CH at *i*Pr), 30.8 (s, C12), 31.9 (s, C11),

dx.doi.org/10.1021/ic500697m | Inorg. Chem. 2014, 53, 6856−6866

Table 2. Crystallographic Data for 2−5

	2·3/2CH_2Cl_2	3·CH_2Cl_2	4·1/2$CHCl_3$	5
chemical formula	$C_{19.5}H_{25}Au_2Cl_5P_2$	$C_{37}H_{46}Cl_6P_4Pt_2$	$C_{40.5}H_{44.5}Cl_{1.5}MoO_4P_4$	$C_{32}H_{45}Cl_2OP_2Rh$
formula weight	892.56	1217.56	868.31	681.47
color	colorless	colorless	red	colorless
crystal system	monoclinic	triclinic	monoclinic	monoclinic
space group	*C*12/*c*1	$P\bar{1}$	*C*12/*c*1	*P*121/*c*1
a (Å)	19.14(3)	8.4920(19)	21.2672(2)	15.138(3)
b (Å)	12.786(14)	10.601(3)	11.072(11)	13.808(3)
c (Å)	22.67(3)	13.737(3)	19.143(2)	16.874(3)
α (deg)	90.0000	85.39(3)	90.0000	90.0000
β (deg)	105.501(14)	73.918(18)	90.793(9)	99.358(19)
γ (deg)	90.0000	79.525(19)	90.0000	90.0000
V (Å^3)	5346(11)	1167.9(5)	4507(5)	3479.9(11)
Z	8	1	4	4
R1	0.0662	0.0583	0.1156	0.2064
wR2	0.1769	0.1558	0.3695	0.5012
GOF	1.117	1.084	1.097	1.102

94.4 (s, Cp* C), 119.6 (d, $^1J_{CP}$ = 8.8 Hz, C1), 122.1 (d, $^3J_{CP}$ = 8.9 Hz, C3), 122.3 (d, $^3J_{CP}$ = 4.0 Hz, C7), 129.9 (dd, $^2J_{CP}$ = 20.8 Hz, $^3J_{CP}$ = 10.7 Hz, C8), 130.9 (s, C2), 137.6−138.3 (m, C5), 139.1−140.3 (m, C10), 142.4 (s, C6), 152.2 (s, C4). $^{31}P\{^1H\}$ NMR (121.5 MHz, $CDCl_3$,): *δ* 11.8 (dd, $^1J_{PRh}$ = 101.5 Hz, PRh), 70.9 (dd, $^2J_{PRh}$ = 3.5 Hz, *i*Pr_2P), $^1J_{PP}$ = 452.4 Hz.

Phosphonic Acid 7. A solution of **1** (0.15 g, 0.50 mmol) in acetonitrile (10 mL) was left open to air for 7 days. Colorless crystals of **7** formed on the walls, which were collected by decantation, washed with acetonitrile, and dried in vacuo (first crop yielded 40 mg (22% yield) of analytically pure material). mp 240−242 °C with decomp. Anal. Calcd for $C_{18}H_{24}O_4P_2$: C 59.05; H, 6.60. Found: C, 59.10; H, 6.68. HRMS (ES$^-$): *m*/*z* 731.2224 ((2M − H)$^-$, $C_{36}H_{47}P_4O_8$ requires 731.2221, 15%), 365.1070 ((M − H)$^-$, $C_{22}H_{23}P_2O_4$ requires 365.1072, 100%), 321.0447 ((M − *i*Pr-2H)$^-$, $C_{15}H_{15}P_2O_4$ requires 321.0446, 20%). IR ν_{max} (KBr disc, cm^{-1}) 3425s (ν_{O-H}), 2971m (ν_{C-H}), 2936w, 1600m, 1443m (δ_{P-C}), 1293s ($\nu_{P=O}$), 1174s ($\nu_{P=O}$), 1126s, 1080m (ν_{P-C}), 989s (ν_{P-OH}), 932s, 702s, 586s.

Dipotassium Salt 7a. Aqueous KOH was added dropwise to a stirred suspension of **7a** in water until slightly alkaline. Removal of volatiles yielded **7a** as white powder (yield quantitative). ^1H NMR (500.1 MHz, D_2O): *δ* 0.61 (6H, dd, $^3J_{HP}$ = 16.7, $^3J_{HH}$ = 7.2 Hz, 2 × CH_3); 1.19 (6H, dd, $^3J_{HP}$ = 15.8, $^3J_{HH}$ = 7.2 Hz, 2 × CH_3), 3.23 (4H, s, H11 and H12), 3.79 (2H, dh, $^3J_{HP}$ = 13.7, $^3J_{HH}$ = 6.8 Hz, 2 × CH at *i*Pr), 7.25 (1H, d, $^3J_{HH}$ = 7.2 Hz, H7), 7.31 (1H, d, $^3J_{HH}$ = 7.3 Hz, H3), 8.00 (1H, dd, $^3J_{HP}$ = 13.1, $^3J_{HH}$ = 7.3 Hz, H2), 8.18 (1H, dd, $^3J_{HP}$ = 14.6, $^3J_{HH}$ = 7.2 Hz, H8). $^{13}C\{^1H\}$ NMR (125.8 MHz, D_2O): *δ* 16.4 (d, $^2J_{CP}$ = 3.9 Hz, 2 × CH_3), 16.7 (d, $^2J_{CP}$ = 4.2 Hz, 2 × CH_3), 26.8 (d, $^1J_{CP}$ = 64.1 Hz, 2 × CH at *i*Pr), 29.2 (s, C11 or C12), 29.3 (s, C-11 or C12), 118.0 (d, $^3J_{CP}$ = 10.8 Hz, C3), 118.9 (d, $^3J_{CP}$ = 13.2 Hz, C7), 124.7 (d, $^1J_{CP}$ = 80.9 Hz, C1), 133.0 (t, $^3J_{CP}$ = 9.6 Hz, C5), 134.8 (d, $^1J_{CP}$ = 160.3 Hz, C9), 136.9 (d, $^2J_{CP}$ = 7.4 Hz, C8), 138.5 (d, $^2J_{CP}$ = 4.6 Hz, C2), 139.0 (t, $^2J_{CP}$ = 10.5 Hz, C10), 152.1 (s, C4), 148.8 (s, C6). ^{31}P NMR: (202.5 MHz, D_2O): *δ* 68.2 (s, *i*Pr_2P(O)), 9.7 (s, P(O)$(OH)_2$). $^{31}P\{^1H\}$ NMR (202.5 MHz, D_2O): *δ* 68.3 (m, *i*Pr_2P(O)), 9.7 (d, $^3J_{PH}$ = 14.7 Hz, P(O)$(OH)_2$). IR ν_{max} (KBr disc, cm^{-1}) 3449m (ν_{O-H}), 2926m (ν_{C-H}), 2620m, 2364m, 1651vs, 1630vs, 1402vs, 1260m, 1168m, 1009s, 832s, 703s. Raman ν_{max} (glass capillary, cm^{-1}) 2929s (ν_{C-H}), 1602s, 1567vs, 1446s, 1417s, 1321vs, 1030s, 588s.

Trisulfide 8 and Disulfide 9. The following procedure gave the highest overall yields of **8** and **9**. To a suspension of S_8 (0.22 g, 6.86 mmol) in toluene (10 mL) was added a solution of **1** (1.0 g, 3.33 mmol) in toluene (20 mL) dropwise, and the mixture was stirred overnight. The resulting yellow solution was filtered, and the volatiles were evaporated in vacuo to give a yellow powder, which was purified by column chromatography on silica gel. Elution with EtOAc/DCM 2:3 gave **9** (0.27g, 0.74 mmol, 22%) and **8** (0.74g, 1.87 mmol, 56%), both as yellow powders.

Characterization Data for 8. mp 262−263 °C. Anal. Calcd for $C_{18}H_{28}P_2S_3$: C 54.52; H, 5.59. Found: C, 54.35; H, 5.36. MS(ES$^+$): *m*/*z* (%) 419.1 ((M+Na)$^+$, 100), 397.0 ((M+H)$^+$, 15); MS(CI$^+$): *m*/*z* (%) 397.0 ((M + H)$^+$, 16), 365.1 ((M−S) + H$^+$), 100), 333.1 ((M−2S) + H$^+$), 14), 300.1 ((M − 3S)$^+$, 14). $^{31}P\{^1H\}$ NMR (121.5 MHz, toluene): *δ* 73.8 (d, PS_3), 55.5 (d, PS*i*Pr_2), $^2J_{PP}$ = 9.4 Hz. $^{31}P\{^1H\}$ SS NMR (MAS 10 kHz, 162.0 MHz): *δ* 69.8 (s), 59.4 (s). After purification, **8** was not soluble in organic solvents, which prevented measurement of ^1H and ^{13}C NMR spectra. Raman (glass capillary, cm^{-1}): *ν* 3053w (*ν*Ar−H), 2977m, 2927s, 2875s (*ν*C−H), 1596m, 1572m, 1438s, 1343vs, 830m, 732m, 690w, 550vs. IR ν_{max} (KBr disc, cm^{-1}) 2971w, 2928w, 2871w (*ν*C−H), 1595m, 1453m, 845m, 732m, 690vs (*ν*P═S) Crystals suitable for X-ray diffraction were grown from EtOAc/DCM eluent.

Characterization Data for 9. mp 240 °C (discolouration), 251−252 °C (melts). Anal. Calcd for $C_{18}H_{28}P_2S_2$: C 59.33; H, 6.09. Found: C, 59.17; H, 5.97. MS (ES$^+$): *m*/*z* (%) 387.15 ((M + Na)$^+$, 100). HRMS (EI$^+$): *m*/*z* (%) calcd for $C_{18}H_{22}P_2S_2$, 364.0638; found, 364.0630. ^1H NMR (300.1 MHz, $CDCl_3$): *δ* 1.42 (dd, $^3J_{HP}$ = 17.4, $^3J_{HH}$ = 7.1 Hz, 6H, 2 × CH_3), 1.60 (dd, $^3J_{HP}$ = 17.0 Hz, $^3J_{HH}$ = 7.2 Hz, 6H, 2 × CH_3), 3.40−3.16 (m, 2H, 2 × CH at *i*Pr), 3.64−3.41 (m, 4H,CH_2), 7.52 (br d, $^3J_{HH}$ = 7.0 Hz, 2H, H3 and H7), 7.83 (dd, $^3J_{HP}$ = 8.2, $^3J_{HH}$ = 7.1 Hz, 1H, H2), 8.14 (dd, $^3J_{HP}$ = 14.0, $^3J_{HH}$ = 7.2 Hz, 1H, H8). $^{13}C\{^1H\}$ NMR (68.9 MHz, CD_2Cl_2): *δ* 17.4−17.5 (m, 4 × CH_3), 24.5 (dd, $^1J_{CP}$ = 29.7, $^2J_{CP}$ = 2.6 Hz, 2 × CH at *i*Pr), 30.8 (d, $^5J_{CP}$ = 1.5 Hz, C11), 31.4−31.6 (m, C12), 110.0 (dd, $^1J_{CP}$ = 55.0 Hz, $^2J_{CP}$ = 10.4 Hz, C1), 120.8 (d, $^3J_{CP}$ = 9.3 Hz, C3), 122.9 (dd, $^3J_{CP}$ = 14.3, $^4J_{CP}$ = 2.3 Hz, C7), 129.3 (dd, $^2J_{CP}$ = 11.2, $^3J_{CP}$ = 5.4 Hz, C8), 133.1−133.7 (m, C10), 133.3 (s, C2), 140.7 (dd, $^1J_{CP}$ = 83.0 Hz, $^2J_{CP}$ = 38.0 Hz, C9), 138.2 (dd, $^3J_{CP}$ = 10.1, $^3J_{CP}$ = 8.6 Hz, C5), 148.5 (d, $^4J_{CP}$ = 1.6 Hz, C6), 153.4 (dd, $^4J_{CP}$ = 2.6, $^4J_{CP}$ = 1.6 Hz, C4). $^{31}P\{^1H\}$ NMR (121.5 MHz, $CDCl_3$): *δ* 5.4 (d, P(*i*Pr_2)$_2$), 69.0 (d, PS_2), $^1J_{PP}$ = 100.1 Hz. Raman (glass capillary, cm^{-1}): *ν* 3054m (*ν*Ar−H), 2929vs, 2883s (*ν*C−H), 1609vs, 1438vs, 1384m, 1345m, 848m, 727m, 684w, 601s (*ν*P═S). IR ν_{max} (KBr disc, cm^{-1}) 2965s, 2926s, 2720w (*ν*C−H), 1737m, 1605w, 1452m, 842m, 805m, 686m. Crystals of **9** suitable for X-ray diffraction were grown by diffusion of hexanes in the solution of **9** in DCM.

Diselenide 10. To a stirred suspension of gray selenium powder (0.53 g, 0.84 mmol) in toluene (10 mL) was added a solution of **1** (1.0 g, 3.33 mmol) in toluene (20 mL) dropwise, and the mixture was then sonicated for 15 min and allowed to stir overnight. The resulting yellow solution was filtered, and the solvent was removed in vacuo to give a bright yellow powder. The crude material was purified by column chromatography on silica gel using EtOAc/DCM 2:3 as the eluent. This afforded **10** as bright yellow needle crystals (1.32 g, 2.88

dx.doi.org/10.1021/ic500697m | Inorg. Chem. 2014, 53, 6856−6866

Table 3. Crystallographic Data for 7−11 and 14

	7	8	9	10	11	14
chemical formula	$C_{18}H_{24}O_4P_2$	$C_{18}H_{22}P_2S_3$	$C_{18}H_{22}P_2S_2$	$C_{18}H_{22}P_2Se_2$	$C_{18}H_{22}P_2Te$	$C_{40}H_{50}Cl_4N_2P_4Zn$
formula weight	366.33	396.50	364.44	458.24	427.92	889.94
color	colorless	colorless	colorless	colorless	red	colorless
crystal system	monoclinic	triclinic	triclinic	triclinic	triclinic	orthorhombic
space group	$P121/c1$	$P\bar{1}$	$P\bar{1}$	$P\bar{1}$	$P\bar{1}$	$P212121$
a (Å)	7.5278(11)	7.9678(13)	8.267(3)	8.3216(12)	8.043(5)	12.941(4)
b (Å)	25.924(4)	14.172(3)	14.8752(10)	15.389(2)	8.499(6)	16.141(4)
c (Å)	9.6195(12)	16.796(3)	16.6453(12)	16.939(2)	14.948(9)	21.948(6)
α (deg)	90.0000	90.762(10)	65.56(5)	64.679(4)	74.381(17)	90.0000
β (deg)	108.860(8)	91.000(7)	79.92(5)	78.050(6)	76.843(16)	90.0000
γ (deg)	90.0000	92.000(8)	81.64(5)	80.604(5)	65.538(17)	90.0000
V (Å^3)	1776.4(4)	1894.9(6)	1828.7(9)	1911.5(5)	887.9(10)	4584(2)
Z	4	4	4	4	2	4
R1	0.0422	0.0705	0.0732	0.0751	0.0434	0.0863
wR2	0.1171	0.1672	0.2748	0.2701	0.1059	0.2243
GOF	1.059	0.921	1.207	0.947	1.084	0.982

mmol, 86%). mp 266−270 °C. Anal. Calcd for $C_{18}H_{22}P_2Se_2$: C 47.18; H, 4.84. Found: C, 47.04; H, 4.79. MS(EI$^+$): m/z (%) 460.0 (M^+, 10), 380.0 ((M − Se)$^+$, 25), 300.1 ((M − 2Se)$^+$, 45), 257.0 ($C_{12}H_8P$-(C_3H_7)P$^+$, 75), 183.0 ($C_{12}H_8P^+$, 40), 152.0 ($C_{12}H_8^+$, 100) 110.9 (SeP^+, 40%). HRMS (EI$^+$): m/z calcd for $C_{18}H_{22}P_2Se_2$, 459.9527; found, 459.9518. ^{1}H NMR (300.1 MHz, CD_2Cl_2): δ 1.37 (dd, $^3J_{HP}$ = 17.4, $^3J_{HH}$ = 7.1 Hz, 6H, 2 × CH_3), 1.61 (dd, $^3J_{HP}$ = 17.1, $^3J_{HH}$ = 7.2 Hz, 6H, 2 × CH_3), 3.66−3.23 (m, 6H, 2 × CH_2 and 2 × CH at *i*Pr), 7.77−7.31 (m, 2H, H3 and H7), 7.92 (dd, $^3J_{HP}$ = 8.2, $^3J_{HH}$ = 7.2 Hz, 1H, H2), 8.04 (dd, $^3J_{HP}$ = 14.1, $^3J_{HH}$ = 7.2 Hz, 1H, H8). ^{13}C{^{1}H} NMR (68.9 MHz, CD_2Cl_2): δ 17.1 (dd, $^2J_{CP}$ = 15.4 Hz, $^3J_{CP}$ = 4.3 Hz, 4 × CH_3), 25.4 (dd, $^1J_{CP}$ = 30.5 Hz, $^2J_{CP}$ = 3.1 Hz, 2 × CH at *i*Pr), 30.9 (d, $^5J_{CP}$ = 1.6 Hz, C12), 31.6 (d, $^5J_{CP}$ = 1.0 Hz, C11), 109.6 (dd, $^1J_{CP}$ = 54.6, $^2J_{CP}$ = 8.4 Hz, C1), 121.1 (d, $^3J_{CP}$ = 9.2 Hz, C3), 122.5 (dd, $^3J_{CP}$ = 14.1, $^4J_{CP}$ = 2.2 Hz, C7), 129.4 (dd, $^2J_{CP}$ = 12.2, $^3J_{CP}$ = 5.0 Hz, C8), 133.1 (dd, $^2J_{CP}$ = 13.7, $^2J_{CP}$ = 10.3 Hz, C10), 134.1 (s, C2), 138.1 (t, $^3J_{CP}$ = 9.0 Hz, C5), 139.8 (dd, $^1J_{CP}$ = 62.5, $^2J_{CP}$ = 32.5 Hz, C9), 149.4−148.7 (m, C6), 154.0 (dd, $^4J_{CP}$ = 2.7, $^5J_{CP}$ = 1.2 Hz, C4). ^{31}P{^{1}H} NMR (121.5 MHz, CD_2Cl_2): δ −0.52 (d, P(*i*Pr)$_2$), 5.9 (d with ^{77}Se satellites, $^1J_{PSe}$ = 693.7 Hz, PSe_2), $^1J_{PP}$ = 150.0 Hz. ^{77}Se NMR (51.5 MHz, CD_2Cl_2): δ 170.7 (br d, $^1J_{SeP}$ = 693.5 Hz). Raman (glass capillary, cm^{-1}): ν 3051m (νAr−H), 2925s, 2875vs (νC−H), 1608s, 1437vs, 1385m, 1344m, 847m, 726m, 597s (νP═Se), 538m. IR ν_{max} (KBr disc, cm^{-1}) 2962w, 2905w (νC−H), 1605m, 1450m, 1381m, 1213m, 1036m, 842m, 606s (νP═Se), 537vs. Crystals suitable for X-ray diffraction were grown from DCM.

Telluride 11. To a stirred suspension of tellurium powder (0.45 g, 3.46 mmol) in toluene (10 mL) was added a solution of **1** (1.0 g, 3.33 mmol) in toluene (20 mL) dropwise. The mixture was then sonicated for 30 min, heated at reflux for 30 min, and stirred overnight at room temperature. The resulting red solution was filtered, and the solvent was removed in vacuo to give a bright red solid. Crystallization from toluene afforded **11** as red platelet crystals (60 mg, 4%) suitable for X-ray diffraction. The small amount of material available and rapid thermal decomposition precluded further characterization.

X-ray Experimental. Tables 2 and 3 list details of data collections and refinements. Data for compounds **2**, **4**, **5**, **8**, and **10** was collected at −148(1) °C using a Rigaku SCX mini and Mo Kα radiation, λ = 0.71075 Å. Data for compounds **3**, **11**, and **14** was collected at −180(1) °C using a Rigaku MM007 high brilliance RA generator and Mercury CCD system using Mo Kα radiation, λ = 0.71075 Å. Data for compound **7** was collected at −148(1) °C using a Rigaku Saturn70 diffractometer and Mo Kα radiation, λ = 0.71075 Å. Data for compound **9** was collected at −100(1) °C using a Rigaku MM007 high brilliance RA generator and a Pilatus detector using Cu Kα radiation, λ = 1.54184 Å. Intensities were corrected for Lorentz-polarization and for absorption. The structures were solved by direct methods and expanded using Fourier techniques. The non-hydrogen atoms were refined anisotropically. Hydrogen atoms were refined using the riding model. The data were collected and processed using CrystalClear.[29] All calculations were performed using the Crystal-Structure crystallographic software package[30] except for refinement, which was performed using SHELXL-97.[31]

The structures **4** and **5**, although satisfactory for proof of connectivity, are of low quality. In both cases, repeated attempts yielded very poor crystals, often highly twinned and with high degrees of solvation. The results presented here were from the best samples measured after several attempts. Thin platelets were used for the final determinations of **5**.

Computational Details. Geometries were fully optimized at the B3LYP/6-31G+* level[32] of density functional theory (DFT), together with a fine integration grid (75 radial shells with 302 angular points per shell). For Se, the 962(d) all-electron basis according to Binning and Curtiss[33] was used, whereas for Te, the Stuttgart−Dresden (SDD) effective core potential along with its double-ζ valence basis set[34] was employed (augmented with a set of d-polarization functions with exponent 0.237).[35] Where available, solid-state structures were used as starting points for the optimizations. For selected compounds (**1**, **2**, **3**, **5**, **9**, and **13**), the minimum character was confirmed through calculation of the harmonic vibrational frequencies, which were all real. All computations were performed using the Gaussian03 suite of programs.[36] Optimized coordinates can be found in the Supporting Information.

■ ASSOCIATED CONTENT

Supporting Information

CIF files for **2**−**5**, **7**−**11**, and **14** and additional computational details including Cartesian coordinates of all computed structures. This material is available free of charge via the Internet at http://pubs.acs.org.

■ AUTHOR INFORMATION

Corresponding Author

*E-mail: pk7@st-andrews.ac.uk. Fax: +44 1334 463808. Phone: +44 1334 467304.

Notes

The authors declare no competing financial interest.

■ ACKNOWLEDGMENTS

We thank C. E. R. Horsburgh at the University of St Andrews and the National Mass Spectrometry Service Center at the University of Swansea for measurement of mass spectra and J. Griffith for measurements of solid-state NMR spectra. We

thank the EaStChem, EPSRC, and the COST actions CM0802 PhoSciNet and CM1302 SIPs for financial support. M.B. wishes to thank H. Früchtl for technical assistance.

REFERENCES

(1) For a recent perspective, see Mathey, F. *Dalton Trans.* **2007**, 1861−1868.
(2) For recent reviews, see (a) Aktas, H.; Slootweg, J. C.; Lammertsma, K. *Angew. Chem., Int. Ed.* **2010**, *49*, 2102−2113. (b) Weber, L. *Eur. J. Inorg. Chem.* **2007**, 4095−4117. (c) Lammertsma, K.; Vlaar, M. J. M. *Eur. J. Org. Chem.* **2002**, 1127−1138. (d) Mathey, F.; Huy, N. H. T.; Marinetti, A. *Helv. Chim. Acta* **2001**, *84*, 2938−2955.
(3) Burg, A. B.; Mahler, W. *J. Am. Chem. Soc.* **1961**, *83*, 2388−2389.
(4) (a) Shah, S.; Protasiewicz, J. D. *Chem. Commun.* **1998**, 1585−1586. (b) Shah, S.; Yap, G. P. A.; Protasiewicz, J. D. *J. Organomet. Chem.* **2000**, *608*, 12−20.
(5) (a) Armbrust, R.; Sanchez, M.; Reau, R.; Bergstrasser, U.; Regitz, M.; Bertrand, G. *J. Am. Chem. Soc.* **1995**, *117*, 10785−10786. (b) Sanchez, M.; Reau, R.; Marsden, C. J.; Regitz, M.; Bertrand, G. *Chem.—Eur. J.* **1999**, *5*, 274−279.
(6) (a) Protasiewicz, J. D. *Eur. J. Inorg. Chem.* **2012**, 4539−4549. (b) Shah, S.; Protasiewicz, J. D. *Coord. Chem. Rev.* **2000**, *210*, 181−201.
(7) Surgenor, B. A.; Bühl, M.; Slawin, A. M. Z.; Woollins, J. D.; Kilian, P. *Angew. Chem., Int. Ed.* **2012**, *51*, 10150−10153.
(8) (a) Partyka, D. V.; Washington, M. P.; Updegraff, J. B., III; Woloszynek, R. A.; Protasiewicz, J. D. *Angew. Chem., Int. Ed.* **2008**, *47*, 7489−7492. (b) Dube, J. W.; Macdonald, C. L. B.; Ragogna, P. J. *Angew. Chem., Int. Ed.* **2012**, *51*, 13026−13030. (c) Scheer, M.; Kuntz, C.; Stubenhofer, M.; Zabel, M.; Timoshkin, A. Y. *Angew. Chem., Int. Ed.* **2010**, *49*, 188−192. (d) Vlaar, M. J. M.; de Kanter, F. J. J.; Schakel, M.; Lutz, M.; Spek, A. L.; Lammertsma, K. *J. Organomet. Chem.* **2001**, *617−618*, 311−317. (e) King, R. B.; Wu, F.-J.; Holt, E. M. *J. Am. Chem. Soc.* **1988**, *110*, 2775−2782.
(9) The Wiberg bond indices (WBI) are a measure for the covalent character of the bond and adopts values close to 1 and 2 for true single and double bonds, respectively; see Wiberg, K. B. *Tetrahedron* **1968**, *24*, 1083−1096.
(10) Stefanescu, D. M.; Yuen, H. F.; Glueck, D. S.; Golen, J. A.; Zakharov, L. N.; Incarvito, C. D.; Rheingold, A. L. *Inorg. Chem.* **2003**, *42*, 8891−8901.
(11) Ekubo, A. T.; Elsegood, M. R. J.; Lake, A. J.; Smith, M. B. *Inorg. Chem.* **2010**, *49*, 3703−3705.
(12) Le Floch, P.; Marinetti, A.; Ricard, L.; Mathey, F. *J. Am. Chem. Soc.* **1990**, *112*, 2407−2410.
(13) Rosenberg, L. *Coord. Chem. Rev.* **2012**, *256*, 606−626.
(14) For a review, see Gilheany, D. G. *Chem. Rev.* **1994**, *94*, 1339−1374.
(15) Dube, J. W.; Macdonald, C. L. B.; Ellis, B. D.; Ragogna, P. J. *Inorg. Chem.* **2013**, *52*, 11438−11449.
(16) For an example of a relevant iron complex, see (a) Cowley, A. H.; Decken, A.; Norman, N. C.; Krüger, C.; Lutz, F.; Jacobsen, H.; Ziegler, T. *J. Am. Chem. Soc.* **1997**, *119*, 3389−3390. (b) Cowley, A. H.; Kilduff, J. E.; Lasch, J. G.; Norman, N. C.; Pakulski, M.; Ando, F.; Wright, T. C. *J. Am. Chem. Soc.* **1983**, *105*, 7751−7752.
(17) Kilgore, U. J.; Fan, H.; Pink, M.; Urnezius, E.; Protasiewicz, J. D.; Mindiola, D. J. *Chem. Commun.* **2009**, 4521−4523.
(18) (a) Sanchez, M.; Reau, R.; Dahan, F.; Regitz, M.; Bertrand, G. *Angew. Chem., Int. Ed.* **1996**, *35*, 2228−2230. (b) Sanchez, M.; Reau, R.; Gornitzka, H.; Dahan, F.; Regitz, M.; Bertrand, G. *J. Am. Chem. Soc.* **1997**, *119*, 9720−9728.
(19) Kilian, P.; Slawin, A. M. Z.; Woollins, J. D. *Chem. Commun.* **2003**, 1174−1175.
(20) Reed, A. E.; Curtiss, F.; Weinhold, L. A. F. *Chem. Rev.* **1988**, *88*, 899−926.
(21) Standard single P−P bond distance is 2.22 ± 0.05 Å.
(22) For a review, see Yoshifuji, M. *J. Organomet. Chem.* **2000**, *611*, 210−216.
(23) Kilian, P.; Slawin, A. M. Z. *Dalton Trans.* **2007**, 3289−3296.
(24) Kilian, P.; Parveen, S.; Fuller, A. L.; Slawin, A. M. Z.; Woollins, J. D. *Dalton Trans.* **2008**, 1908−1916.
(25) Le Floch, P.; Mathey, F. *Synlett* **1990**, 171−172.
(26) Wawrzyniak, P.; Fuller, A. L.; Slawin, A. M. Z.; Kilian, P. *Inorg. Chem.* **2009**, *48*, 2500−2506.
(27) An interesting parallel to this is found in the reductive coupling protocol used in the preparation of diphosphenes from organodichlorophosphines, where identity of the reducing reagent is also critical and the choice is not always intuitive; for an example, see Twamley, B.; Sofield, C. D.; Olmstead, M. M.; Power, P. P. *J. Am. Chem. Soc.* **1999**, *121*, 3357−3367.
(28) Drew, D.; Doyle, J. R. *Inorg. Synth.* **1972**, *13*, 47−49.
(29) (a) *CrystalClear 1.6*, CrystalClear Software User's Guide: Rigaku Corporation: Tokyo, Japan, 2000. (b) Flugrath, J. W. P. *Acta Crystallogr.* **1999**, *D55*, 1718.
(30) *CrystalStructure 4.0*; Rigaku Corporation: Tokyo, Japan.
(31) Sheldrick, G. M. *Acta Crystallogr.* **2008**, *A64*, 112−122.
(32) (a) Becke, A. D. *J. Chem. Phys.* **1993**, *98*, 5648−5642. (b) Lee, C.; Yang, W.; Parr, R. G. *Phys. Rev. B* **1988**, *37*, 785−789.
(33) Binning, R. C.; Curtiss, L. A. *J. Comput. Chem.* **1990**, *11*, 1206.
(34) (a) Schwerdtfeger, P.; Dolg, M.; Schwarz, W. H. E.; Bowmaker, G. A.; Boyd, P. D. W. *J. Chem. Phys.* **1989**, *91*, 1762−1774. (b) Bergner, A.; Dolg, M.; Kuechle, W.; Stoll, H.; Preuss, H. *Mol. Phys.* **1993**, *80*, 1431−1441.
(35) Huzinaga, S.; Anzelm, J.; Klobukowski, M.; Radzio-Andzelm, E.; Sakai, Y.; Tatewaki, H. *Gaussian Basis Sets for Molecular Calculations*; Elsevier: Amsterdam, The Netherlands, 1984.
(36) Frisch, M. J.; Trucks, G. W.; Schlegel, H. B.; Scuseria, G. E.; Robb, M. A.; Cheeseman, J. R.; Montgomery, J. A., Jr.; Vreven, T.; Kudin, K. N.; Burant, J. C.; Millam, J. M.; Iyengar, S. S.; Tomasi, J.; Barone, V.; Mennucci, B.; Cossi, M.; Scalmani, G.; Rega, N.; Petersson, G. A.; Nakatsuji, H.; Hada, M.; Ehara, M.; Toyota, K.; Fukuda, R.; Hasegawa, J.; Ishida, M.; Nakajima, T.; Honda, Y.; Kitao, O.; Nakai, H.; Klene, M.; Li, X.; Knox, J. E.; Hratchian, H. P.; Cross, J. B.; Bakken, V.; Adamo, C.; Jaramillo, J.; Gomperts, R.; Stratmann, R. E.; Yazyev, O.; Austin, A. J.; Cammi, R.; Pomelli, C.; Ochterski, J. W.; Ayala, P. Y.; Morokuma, K.; Voth, G. A.; Salvador, P.; Dannenberg, J. J.; Zakrzewski, V. G.; Dapprich, S.; Daniels, A. D.; Strain, M. C.; Farkas, O.; Malick, D. K.; Rabuck, A. D.; Raghavachari, K.; Foresman, J. B.; Ortiz, J. V.; Cui, Q.; Baboul, A. G.; Clifford, S.; Cioslowski, J.; Stefanov, B. B.; Liu, G.; Liashenko, A.; Piskorz, P.; Komaromi, I.; Martin, R. L.; Fox, D. J.; Keith, T.; Al-Laham, M. A.; Peng, C. Y.; Nanayakkara, A.; Challacombe, M.; Gill, P. M. W.; Johnson, B.; Chen, W.; Wong, M. W.; Gonzalez, C.; Pople, J. A. *Gaussian 03*, revision E.01; Gaussian, Inc.: Wallingford, CT, 2003.